Molecular characterization of acquired resistance to KRAS G12C inhibition in gastrointestinal cancers

Sandra Misale (misales@mskcc.org)
Memorial Sloan Kettering Cancer Center

Rona Yaeger
Memorial Sloan-Kettering Cancer Center

Riccardo Mezzadra
Memorial Sloan Kettering Cancer Center

Jenna Sinopoli
Memorial Sloan Kettering Cancer Center

Yu Bian
Memorial Sloan Kettering Cancer Center

Michelangelo Marasco
MSKCC

Esther Kaplun
Memorial Sloan Kettering Cancer Center

Yijun Gao
Memorial Sloan Kettering Cancer Center

Huiyong Zhao
Memorial Sloan Kettering Cancer Center

Arnaud Da Cruz Paula
Memorial Sloan Kettering Cancer Center

Yingjie Zhu
Memorial Sloan Kettering Cancer Center

Sydney Bowker
Memorial Sloan Kettering Cancer Center

Qing Chang
Memorial Sloan Kettering Cancer Center

Besnik Qeriqi
MSKCC

Britta Weigelt
Memorial Sloan Kettering Cancer Center https://orcid.org/0000-0001-9927-1270

Hirak Der-Torossian
Mirati Therapeutics, Inc.

Kenna Anderes

Mirati Therapeutics, Inc.
Nicholas Socci
Memorial Sloan Kettering Cancer Center
Jinru Shia
Memorial Sloan Kettering Cancer Center https://orcid.org/0000-0002-4351-2511
Greg Riely
MSKCC
Yonina Murciano-Goroff
Memorial Sloan-Kettering Cancer Center
Bob Li
Memorial Sloan Kettering Cancer Center https://orcid.org/0000-0001-6661-8733
James Christensen
Mirati Therapeutics, Inc.
Jorge Reis-Filho
Memorial Sloan Kettering Cancer Center https://orcid.org/0000-0003-2969-3173
David Solit
Memorial Sloan Kettering Cancer Center https://orcid.org/0000-0002-6614-802X
Elisa de Stanchina
Antitumor Assessment Core Facility - Molecular Pharmacology Program, Memorial Sloan Kettering Cancer, New York, NY
Scott Lowe
Memorial Sloan Kettering Cancer Center and Howard Hughes Medical Institute https://orcid.org/0000-0002-5284-9650
Neal Rosen
https://orcid.org/0000-0002-8307-654X

Biological Sciences - Article

Keywords:

Posted Date: January 12th, 2022

DOI: https://doi.org/10.21203/rs.3.rs-1236956/v1

Abstract

KRAS G12C inhibitors, such as sotorasib, have rapidly moved through clinical development and are poised to transform care of patients with KRAS G12C mutant cancers, in particular non-small cell lung cancer (NSCLC) and colorectal cancer (CRC). Clinical efficacy is achieved in NSCLC as a single agent and in CRC in combination with anti-EGFR monoclonal antibodies, however, secondary resistance impairs the effects of KRAS G12C blockade. In this work, we sought to determine the mechanisms of acquired resistance to concomitant KRAS-EGFR inhibition. In cell lines, patient-derived xenograft, and patient samples, a heterogeneous pattern of putative resistance alterations expected primarily to prevent inhibition of ERK signalling by drug can be detected at progression. Serial analysis of patient blood samples on treatment demonstrates that most of these alterations are detected at a low frequency that does not increase substantially and sometimes disappears over time, with the exception of KRAS G12C amplification which rises in step with tumour marker levels and clinical progression. Here we show that a CRC cell line that acquired resistance to sotorasib-cetuximab combination through KRAS G12C amplification became addicted to these agents and undergoes oncogene-induced senescence upon drug withdrawal. Accordingly, the KRAS G12C signal in circulating DNA from relapsed patients harbouring G12C amplification rapidly recedes upon treatment holiday. These data indicate that KRAS G12C amplification is a recurrent resistance mechanism to KRAS-EGFR co-inhibition and suggest a potential therapeutic vulnerability, whereby therapies that target this senescence response at drug withdrawal may overcome resistance to KRAS G12C-EGFR inhibition.

Full Text

KRAS is the most commonly mutated oncogene in human cancer[1]. It acts as a signalling switch that, when bound to GTP, orchestrates a program of cell proliferation and survival. Until recently, efforts to target KRAS have been unsuccessful due to its small binding pocket, high affinity for GTP, and redundant mechanisms of posttranslational processing. The development of allele specific KRAS G12C inhibitors that trap KRAS in the inactive, GDP-bound state[2,3] led to a paradigm change, with clinical responses in 30-50% of non-small cell lung cancer (NSCLC) patients harbouring KRAS G12C mutations [4,5].

These agents are not as effective in colorectal cancers (CRC) with KRAS G12C mutation. We have previously shown that the activity of these drugs in KRAS G12C CRC is limited because activation of epidermal growth factor receptor (EGFR) reactivates ERK signalling and consequently combinatorial KRAS G12C and EGFR inhibition more effectively targets KRAS G12C CRC[6]. Early trial data provide clinical support for this observation: the response rate for sotorasib was 7-10% in CRC[7] and, in the first report of sotorasib plus the EGFR antibody panitumumab, the response rate was 27%[8]. For adagrasib monotherapy, it was ~20% and, for adagrasib with the EGFR antibody cetuximab, it increased to ~40%[9]. Based on these data, these KRAS G12C and EGFR antibody combination treatments are being evaluated in registrational, phase 3 trials.

Nonetheless, patients treated with these agents eventually acquire resistance and the response to single agent or combination treatment is brief. Several studies have characterized resistance to KRAS G12C monotherapy[10-12]. Remarkably, these alterations are highly heterogeneous, including KRAS, BRAF, or MEK mutations, as well as gene amplifications and fusions, and circulating tumour DNA (ctDNA) analysis typically identifies multiple resistance alterations in the same patient.

To identify mechanisms of resistance to the combination of KRAS G12C and EGFR inhibitors, we grew the CRC cell lines C106 and RW7213, both of which are sensitive to this treatment[6] in drugs until the emergence of secondary resistance **(Figure 1a)**. Treatment with sotorasib 3mM and cetuximab 50mg/mL led to massive cell death of both cell lines with few viable cells. Cells were therefore subjected to increasing doses of sotorasib (from 0.1mM to 3mM) with cetuximab 50mg/mL to generate resistance **(Extended Data Figure 1a)**. Resistant sublines grew well in drugs after a period of 4 months for C106 cells and 2 months for RW7213 cells **(Extended Data Figure 1a, 1b, 1d)**.

Both resistant sublines expressed higher RAS-GTP levels than parental cells and drug treatment led to incomplete inhibition of RAS-GTP **(Extended Data Figures 1c, 1e)**. Drug treatment of C106 cells failed to suppress activity of downstream effectors in the RAS/ERK pathway, whereas RW7213 resistant cells experienced a reduction in pathway activity but continued to have high levels of phospho-MEK and phospho-ERK due to elevated baseline pathway activation. Targeted sequencing of the resistant sublines using MSK-IMPACT[13] identified acquired NRAS G12D mutation in C106 cells and KRAS G12C amplification in RW7213 cells **(Extended Data Figure Table 1)**. Single cell sequencing of the C106 resistant subline indicated that the NRAS G12D mutation occurred in the same cells bearing the KRAS G12C alteration **(Figure 1b)**. The variant allelic frequency (VAF) of the NRAS mutation suggested allelic imbalance with an acquired gain of the NRAS allele, which was confirmed by bulk targeted exome sequencing (MSK-IMPACT). This seems to be a late event occurring in a subpopulation of the cells. More than 20 copies of KRAS per cell were detected in resistant RW7213 cells with fluorescence in situ hybridization **(Figure 1c)**. In parallel, a KRAS G12C mutant CRC patient-derived xenograft (PDX) model (CLR113) that was initially sensitive to sotorasib and cetuximab combination treatment[6] **(Extended Data Figure 1f)** developed acquired resistance after about 10 months that was associated with KRAS G12C amplification, BRAF K601E, and RAF1 S259F acquired alterations **(Figure 1d)**. These data indicate that multiple resistance mechanisms can contribute to the survival of KRAS G12C mutant cells and that KRAS G12C amplification is a recurrent alteration at resistance.

To evaluate potential resistance mechanisms to KRAS G12C inhibitor (KRAS G12Ci) and anti-EGFR antibody (EGFRi) in patients, we collected circulating free DNA (cfDNA) from eleven CRC patients treated with combination treatment who initially experienced tumour regression and then developed either radiographic (RECIST) or clinical progression **(Extended Data Figure 2 and Extended Data Table 2)**. Emergent alterations identified at resistance **(Figure 1e)** included KRAS G12C amplification, KRAS mutations (G12A/D/F/LR/S/V, H95L/Q/R, and Y96D/H/N), NRAS mutation (Q61K/R), downstream ERK pathway alterations (BRAF mutations/fusions, MEK1 mutations), RTK activation (MET amplification/fusion, RET fusion, EGFR mutations), and MYC amplification. Similar to what was

previously reported for resistance to KRAS G12C inhibitor monotherapy and in accordance with our preclinical models treated with sotorasib-cetuximab combination, multiple resistance-associated alterations were identified in individual patients, with the majority predicted to prevent inhibition of ERK signalling by drug[12].

Similar to resistance alterations to KRAS G12C inhibitor monotherapy[10,11], all acquired alterations were identified at low VAF, at one-tenth or one-hundredth of the frequency of alterations identified at baseline. To better understand clonal dynamics of resistance in gastrointestinal cancers, cfDNA was serially collected during treatment and sequenced about every six weeks in four CRC, one pancreatic cancer, and one small bowel cancer patients **(Figure 2, Extended Data Figure 3, and Extended Data Table 3)**. Longitudinal analysis confirmed the emergence of multiple resistance alterations. Resistant alterations often emerged many weeks before the development of clinical resistance and remained at a low frequency, largely <1% VAF, while the baseline alterations and tumour marker (CEA for CRC and small bowel cancer patients or Ca19-9 for pancreatic cancer patient) rose higher during treatment. In multiple patients, once resistance was first detected, each successive time point identified new resistance alterations with only modest changes in the VAF of the pre-existing resistant alterations. We did not observe a clonal sweep with emergence of a dominant resistance alteration in any patient. In several patients, the VAF of the putative resistance alterations actually decreased and became undetectable despite continued treatment. These included alterations expected to cause resistance to a KRAS G12C inhibitor, such as the KRAS G13D, NRAS Q61K, and BRAF V600E mutations detected in patient 1 **(Figure 2a)** and the BRAF V600E mutation and BRAF fusion in patient 3 **(Figure 2c)**. These data together suggest that resistant subclones do not grow effectively and are unable to grow out to dominate the population. Indeed, among the many low frequency resistance alterations detected in patients, the only putative resistance genetic event that correlated with tumour marker response was KRAS G12C amplification. Clinical resistance to KRAS G12C inhibition is thus characterized by the accumulation and loss of many low frequency resistance alterations, while KRAS G12C amplification drives a higher portion of the resistance phenotype.

Intrigued by the correlation of KRAS G12C amplification with clinical resistance, we used the RW7213-resistant cells (RW7213-R) harbouring high-grade KRAS G12C amplification to investigate the characteristics of this resistance mechanism. The resistant cells grow well as colonies in medium containing cetuximab and sotorasib, maintaining the same morphology of the parental RW7213 cell line. However, these cells failed to proliferate, acquired a large and flat morphology, and accumulated vacuoles 5 to 7 days after drug withdrawal **(Figure 3a)** suggesting that RW7213-R cells became addicted to the drug combination. The morphological features of these cells are reminiscent of cellular senescence, a tumour suppressive program that can be triggered by excessive oncogenic signaling[14]. In addition to acquiring a proliferative arrest and protection from apoptosis, senescent cells activate a secretory program known as the senescence associated secretory phenotype (SASP)[15,16]. Also in line with a senescent phenotye, RW7213-R cells taken off the drug combination downregulated apoptosis, increased expression of cyclin-dependent kinase inhibitors and uPAR, a marker of senescence[17], and accumulate

cytokines indicative of SASP **(Figure 3b, 3c)**. By contrast, C106-R cells not harbouring KRAS G12C amplification did not exhibit the senescence phenotype or markers (**Extended Data Figure 4**), suggesting that this effect is specific for KRAS G12C amplification. These data suggest that high levels of KRAS signalling, which are needed to drive resistance to the drugs, trigger oncogene-induced senescence upon drug withdrawal. ERK inhibition in these cells by drug treatment is incomplete but re-establishes pathway signalling to a new steady state, similar to active-ERK levels of the parental cells in the absence of drug **(Extended Data Figure 1e)**.

Given the dramatic effect of drug withdrawal in the *in vitro* model, we wondered if KRAS G12C amplification produces a selective disadvantage in patients and monitored the effect of drug withdrawal in three patients with acquired KRAS G12C amplification at resistance. In a pancreatic cancer patient, KRAS G12C inhibitor monotherapy was held for eight days for toxicity at the time of emerging clinical resistance. Analysis of ctDNA before and after drug withdrawal revealed a dramatic reduction in both KRAS G12C and KRAS amplification one week after disrupting treatment **(Figure 4a)**. A similar result was observed in CRC patients 1 and 5, who both harboured KRAS G12C mutant CRC that had developed multiple resistance alterations, including KRAS G12C amplification **(Figure 1e, 2a)**. Again, comparison of ctDNA from before and about 4 weeks after drug withdrawal in each of these patients showed a 2-fold reduction of the signal from KRAS amplification. By contrast, the relative frequency of the other pre-existing alterations and emergent mutations remained mostly unchanged (**Figure 4b, 4c**). Together these data show that KRAS G12C amplification is a mechanism of secondary resistance that shows fitness only in the presence of the selective pressure mediated by drug treatment.

Here we report the genetic mechanisms of secondary resistance to concomitant EGFR and KRAS G12C blockade in KRAS G12C mutant CRC. In agreement with previous studies, our patients show sub-clonal heterogeneity and low variant allele frequency. This may be due in part to the evaluation of ctDNA as this method exposes tumour heterogeneity more than single biopsy specimens[18]. However, our data suggest that low clonal fitness may provide the driving pressure for the accumulation of alterations as resistance alterations appear and disappear during continued therapy. Further, our data suggest that a small fraction of cells may be sufficient to drive clinical resistance. This concept is in line with recent studies of metastatic behaviour where, for example, single cell RNA sequencing of small cell lung cancers identified a rare population of stem-like cells that appears to drive metastatic outcomes in this cancer[19].

In contrast to the low frequency of other resistance mechanisms, we identify KRAS G12C amplification as a recurrent resistance mechanism that tracks with tumour markers and response. KRAS G12C amplification engages the senescence program as it results in supra-high levels of ERK signalling when drug is removed. We show that amplified KRAS G12C recedes in the absence of drug in patients. Similar to our findings, BRAF amplification upon RAF inhibitor resistance can be modulated by intermittent treatment[20]. Copy number changes may provide a more rapid means to modulate oncogene activity as we find that KRAS G12C amplification emerges faster than resistance mutations in cell lines and that amplification carried on extrachromosomal DNA/double minutes, as seen in the RW7213-R cells, may be quickly lost at times of stress[21]. Our data suggest that this drop in the cell free DNA is likely due to the

acquisition of a senescent phenotype in cancer cells, therefore intermittent treatment would probably just favour the survival of KRAS G12C amplified cells. Moreover, the heterogeneity of resistance mechanisms we and others identified suggests that intermittent dosing will not be sufficient to overcome resistance. Our data instead raise the potential of novel therapeutic approaches that exploit vulnerabilities due to the senescence program during periods of drug withdrawal to target resistant cells more broadly. SASP chemokines can recruit immune cells suggesting the potential to target resistant cancer cells with immune checkpoint inhibitors[22-25]. Also, drug withdrawal can potentially be combined with senolytic approaches[26] to facilitate tumour clearance, such as through inhibition of mTOR signaling[27] or antiapoptotic mediators[28]. Moreover, senescence-driven expression of uPAR could also become a target for CART cell therapy[29].

Further studies will provide important insights on how to effectively target KRAS G12C mutant cancers that developed secondary resistance to KRAS G12C inhibitors as single agents and in combination.

Declarations

Acknowledgements

Supported by National Institutes of Health R01 CA233736 (R.Y., N.R.), U54 OD020355 (E. DS.), and Cancer Center Core Grant P30 CA 008748. R.M. is a Cancer Research Institute Irvington Fellow supported by the Cancer Research Institute (CRI Award 3441). Y.R.M-G. is supported by the Kristina M. Day Young Investigator Award from Conquer Cancer, the ASCO Foundation, and received training through an NIH K30 institutional grant (CTSA UL1TR00457). This research is the responsibility of the authors and does not necessarily represent the official views of the National Institutes of Health.

Authors contributions

Conceptualization: R.Y., R.M., S.W.L., N.R. and S.M. Methodology and Analysis: R.M., Y.B., M.M., E.K., Y.G., HY.Z., A.DCP., Y.Z., S.B., Q.C., B.Q., B.W., H.DT., K.A., N.D.S., J.S. Writing – Original Draft: R.Y., R.M., S.W.L., N.R. and S.M. Writing – Review & Editing: R.Y., R.M., Y.R.M-G., B.T.L., S.W.L., N.R. and S.M. Supervision: R.Y., G.R., B.T.L., J.G.C., J.R.F., D.B.S, E.DS., S.W.L., N.R. and S.M. Funding Acquisition: R.Y., N.R., S.W.L.

Competing interest declaration

R.Y. has served as an advisor for Natera, Array BioPharma/Pfizer, and Mirati Therapeutics and has received research support to her institution from Array BioPharma/Pfizer, Boehringer Ingelheim, and Mirati Therapeutics. H.D., K.A., J.C.G. are employees of Mirati Therapeutics. G.R. has been an uncompensated consultant to Daiichi, Pfizer, Merck, Verastem, Novartis, and Mirati and has institutional research support from Mirati, Takeda, Merck, Roche, Pfizer, and Novartis. Y.R.M-G. has received honoraria from Virology Education and has received travel, accommodation and expenses from AstraZeneca. B.T.L. has served as a consultant/advisory board member for Roche, Biosceptre International, Thermo Fisher Scientific, Mersana Therapeutics, Hengrui Therapeutics, Guardant Health and has received research funds to his

institution from Genentech, Daiichi Sankyo, Hengrui Therapeutics, Illumina, BioMed Valley Discoveries, AstraZeneca, GRAIL, and Amgen. J.S.R-F. is a member of the scientific advisory board (with paid honoraria) of Volition Rx, Paige.AI, Invicro, Roche, Genentech, and Ventana, and a consultant with paid fees of Goldman Sachs Merchant Banking. D.B.S. has consulted with and received honoraria from Pfizer, Loxo Oncology, Lilly Oncology, Vivideon Therapeutics, Q.E.D. Therapeutics and Illumina. N.R. is on the scientific advisory board (SAB) of Chugai, BeiGene, Fortress Biotech, Daiichi-Sankyo, AstraZeneca, F-Prime, Zai Lab, Arvinas, and Array BioPharma; and he is a past SAB member of Millennium-Takeda, Kadmon, Kura Oncology, and Araxes. N.R. is also a consultant to Novartis Biomed, Boehringer Ingelheim, Tarveda, Foresite Capital, Array BioPharma, and Revolution Medicines; and in recent years has also consulted with Eli Lilly, Merrimack, Kura Oncology, Araxes, and Kadmon. N.R. owns equity in BeiGene, Zai Lab, Fortress Biotech, Kura Oncology, Araxes, Kadmon, and Effector. S.M. has served as a consultant for Boehringer Ingelheim. All other authors declare no potential conflicts.

Additional information

Corresponding Authors: Rona Yaeger (yaegerr@mskcc.org) and Sandra Misale (misales@mskcc.org)

References

1 Zehir, A. *et al.* Mutational landscape of metastatic cancer revealed from prospective clinical sequencing of 10,000 patients. *Nat Med* **23**, 703-713, doi:10.1038/nm.4333 (2017).

2 Ostrem, J. M., Peters, U., Sos, M. L., Wells, J. A. & Shokat, K. M. K-Ras(G12C) inhibitors allosterically control GTP affinity and effector interactions. *Nature* **503**, 548-551, doi:10.1038/nature12796 (2013).

3 Lito, P., Solomon, M., Li, L. S., Hansen, R. & Rosen, N. Allele-specific inhibitors inactivate mutant KRAS G12C by a trapping mechanism. *Science* **351**, 604-608, doi:10.1126/science.aad6204 (2016).

4 Skoulidis, F. *et al.* Sotorasib for Lung Cancers with. *N Engl J Med* **384**, 2371-2381, doi:10.1056/NEJMoa2103695 (2021).

5 G., R. *et al.* 99O_PR - KRYSTAL-1: Activity and Preliminary Pharmacodynamic (PD) Analysis of Adagrasib (MRTX849) in Patients (Pts) With Advanced Non-Small- Cell Lung Cancer (NSCLC) Harboring KRASG12C Mutation. *Journal of Thoracic Oncology (2021) 16 (suppl_4): S748-S802.* (2021).

6 Amodio, V. *et al.* EGFR Blockade Reverts Resistance to KRAS. *Cancer Discov* **10**, 1129-1139, doi:10.1158/2159-8290.CD-20-0187 (2020).

7 Fakih, M. G. *et al.* Sotorasib for previously treated colorectal cancers with KRAS. *Lancet Oncol*, doi:10.1016/S1470-2045(21)00605-7 (2021).

8 Fakih, M. G. *et al.* 434P CodeBreaK 101 subprotocol H: Phase Ib study evaluating combination of sotorasib (Soto), a KRASG12C inhibitor, and panitumumab (PMab), an EGFR inhibitor, in advanced KRAS

p.G12C-mutated colorectal cancer (CRC). *Annals of Oncology* **Volume 32**, S551, doi:10.1016/j.annonc.2021.08.955 (2021).

9 Weiss, J. *et al.* LBA6 KRYSTAL-1: Adagrasib (MRTX849) as monotherapy or combined with cetuximab (Cetux) in patients (Pts) with colorectal cancer (CRC) harboring a KRASG12C mutation. *Annals of Oncology* **Volume 32**, S1294, doi:10.1016/j.annonc.2021.08.2093. (2021).

10 Tanaka, N. *et al.* Clinical Acquired Resistance to KRAS. *Cancer Discov* **11**, 1913-1922, doi:10.1158/2159-8290.CD-21-0365 (2021).

11 Awad, M. M. *et al.* Acquired Resistance to KRAS G12C Inhibition in Cancer. *N Engl J Med* **384**, 2382-2393, doi:10.1056/NEJMoa2105281 (2021).

12 Zhao, Y. *et al.* Diverse alterations associated with resistance to KRAS(G12C) inhibition. *Nature* **599**, 679-683, doi:10.1038/s41586-021-04065-2 (2021).

13 Cheng, D. T. *et al.* Memorial Sloan Kettering-Integrated Mutation Profiling of Actionable Cancer Targets (MSK-IMPACT): A Hybridization Capture-Based Next-Generation Sequencing Clinical Assay for Solid Tumor Molecular Oncology. *J Mol Diagn* **17**, 251-264, doi:10.1016/j.jmoldx.2014.12.006 (2015).

14 Serrano, M., Lin, A. W., McCurrach, M. E., Beach, D. & Lowe, S. W. Oncogenic ras provokes premature cell senescence associated with accumulation of p53 and p16INK4a. *Cell* **88**, 593-602, doi:10.1016/s0092-8674(00)81902-9 (1997).

15 Sharpless, N. E. & Sherr, C. J. Forging a signature of in vivo senescence. *Nat Rev Cancer* **15**, 397-408, doi:10.1038/nrc3960 (2015).

16 Collado, M. & Serrano, M. The power and the promise of oncogene-induced senescence markers. *Nat Rev Cancer* **6**, 472-476, doi:10.1038/nrc1884 (2006).

17 Ruscetti, M. *et al.* NK cell-mediated cytotoxicity contributes to tumor control by a cytostatic drug combination. *Science* **362**, 1416-1422, doi:10.1126/science.aas9090 (2018).

18 Strickler, J. H. *et al.* Genomic Landscape of Cell-Free DNA in Patients with Colorectal Cancer. *Cancer Discov* **8**, 164-173, doi:10.1158/2159-8290.CD-17-1009 (2018).

19 Chan, J. M. *et al.* Signatures of plasticity, metastasis, and immunosuppression in an atlas of human small cell lung cancer. *Cancer Cell* **39**, 1479-1496 e1418, doi:10.1016/j.ccell.2021.09.008 (2021).

20 Das Thakur, M. *et al.* Modelling vemurafenib resistance in melanoma reveals a strategy to forestall drug resistance. *Nature* **494**, 251-255, doi:10.1038/nature11814 (2013).

21 Song, K. *et al.* Plasticity of extrachromosomal and intrachromosomal BRAF amplifications in overcoming targeted therapy dosage challenges. *Cancer Discov*, doi:10.1158/2159-8290.CD-20-0936

(2021).

22 Gasek, N. S., Kuchel, G. A., Kirkland, J. L. & Xu, M. Strategies for Targeting Senescent Cells in Human Disease. *Nat Aging* **1**, 870-879, doi:10.1038/s43587-021-00121-8 (2021).

23 Xue, W. *et al.* Senescence and tumour clearance is triggered by p53 restoration in murine liver carcinomas. *Nature* **445**, 656-660, doi:10.1038/nature05529 (2007).

24 Kang, T. W. *et al.* Senescence surveillance of pre-malignant hepatocytes limits liver cancer development. *Nature* **479**, 547-551, doi:10.1038/nature10599 (2011).

25 Kale, A., Sharma, A., Stolzing, A., Desprez, P. Y. & Campisi, J. Role of immune cells in the removal of deleterious senescent cells. *Immun Ageing* **17**, 16, doi:10.1186/s12979-020-00187-9 (2020).

26 Kirkland, J. L. & Tchkonia, T. Senolytic drugs: from discovery to translation. *J Intern Med* **288**, 518-536, doi:10.1111/joim.13141 (2020).

27 Wang, C. *et al.* Inducing and exploiting vulnerabilities for the treatment of liver cancer. *Nature* **574**, 268-272, doi:10.1038/s41586-019-1607-3 (2019).

28 Yosef, R. *et al.* Directed elimination of senescent cells by inhibition of BCL-W and BCL-XL. *Nat Commun* **7**, 11190, doi:10.1038/ncomms11190 (2016).

29 Amor, C. *et al.* Senolytic CAR T cells reverse senescence-associated pathologies. *Nature* **583**, 127-132, doi:10.1038/s41586-020-2403-9 (2020).

30 Zill, O. A. *et al.* The Landscape of Actionable Genomic Alterations in Cell-Free Circulating Tumor DNA from 21,807 Advanced Cancer Patients. *Clin Cancer Res* **24**, 3528-3538, doi:10.1158/1078-0432.CCR-17-3837 (2018).

31 Odegaard, J. I. *et al.* Validation of a Plasma-Based Comprehensive Cancer Genotyping Assay Utilizing Orthogonal Tissue- and Plasma-Based Methodologies. *Clin Cancer Res* **24**, 3539-3549, doi:10.1158/1078-0432.CCR-17-3831 (2018).

32 Pellegrino, M. *et al.* High-throughput single-cell DNA sequencing of acute myeloid leukemia tumors with droplet microfluidics. *Genome Res* **28**, 1345-1352, doi:10.1101/gr.232272.117 (2018).

33 Martin, M. Cutadapt removes adapter sequences from high-throughput sequencing reads. *2011* **17**, 3, doi:10.14806/ej.17.1.200 (2011).

34 Li, H. & Durbin, R. Fast and accurate short read alignment with Burrows-Wheeler transform. *Bioinformatics* **25**, 1754-1760, doi:10.1093/bioinformatics/btp324 (2009).

35 Li, H. *et al.* The Sequence Alignment/Map format and SAMtools. *Bioinformatics* **25**, 2078-2079, doi:10.1093/bioinformatics/btp352 (2009).

36 McKenna, A. *et al.* The Genome Analysis Toolkit: a MapReduce framework for analyzing next-generation DNA sequencing data. *Genome Res* **20**, 1297-1303, doi:10.1101/gr.107524.110 (2010).

Methods

Cell lines and Compounds

RW7213 cell line was cultured in RPMI (Lonza). C106 cell line was cultured in Iscove's modified medium (Lonza). Each media was supplemented with 10% FBS, 2mM L-glutamine, 100U/ml penicillin and 100mg/mL streptomycin. Resistant derivatives were grown in media containing cetuximab (50mg/mL) and sotorasib (3mM). C106 cells were purchased from ECACC, RW7213 were provided by Dr. Diego Arando.

All the cell lines were determined to be mycoplasma free using the Venor® GeM Classic kit (Minerva biolabs) and tested by Short Tandem Repeats profiling at 10 different loci.

Sotorasib and trametinib were purchased from SelleckChem. Cetuximab was purchased from the Pharmacy at Memorial Sloan Kettering Cancer Center.

Cell viability assay

For time course proliferation assays, 1,000 cells were seeded in 96-well culture plates in medium containing 10% FBS. After 24 hours, the indicated concentrations of sotorasib and cetuximab were added to cell in 10% FBS medium (ratio 1:1). Cell viability was assayed with alamarBlue. DMSO-only treated cells were used as control. Assays were performed with eight replicates and were each repeated three times. In all the experiments, plates were incubated at 37°C in 5% $CO_{2.}$

Antibodies and Western blotting

After seeding and drug treatments, cells were washed with cold PBS and lysed in RIPA buffer (Pierce #89901) plus phosphatase and protease inhibitors (Thermo Scientific #1861277, #1861278). Lysates were cleared by centrifugation at 14000rpm at 4°C and quantified using BCA method (Pierce #23224).

Samples were prepared using LDS+Reducing agent Novex buffers (Invitrogen #NP0008, #NP0009). 10 to 20µg of lysates were loaded and run on NuPageTM 4-12% Bis-Tris gels (ThermoFisher #NP0321BOX) followed by transfer to nitrocellulose membranes (Biorad #1620233). Membranes were incubated over night with the indicated antibodies, washed and incubated again for 45 minutes with anti-rabbit or anti-mouse secondary antibodies. Detection was performed using Immobilion Western (Millipore #WBKLS0500).

Primary antibodies were obtained from Cell Signaling Technology and were used at a concentration of 1:1000: anti-p16 (#80772), anti-p21 12D1 (#2947), anti-Actin (#4970), anti-phospho-MEK1/2 S217/221 (#9154), anti-phospho-p44/42 MAPK T202/204 (#9101), anti-total ERK1/2 (#9102), anti-total EGFR

(#2232S), anti-phospho-EGFR Tyr1068 (#3777S) and anti-Vinculin (#13901S). Anti-CyclinD1 antibody was purchased from Thermo-Scientific (PA516777) and used at 1:1000 dilution. Anti-KRAS and anti-NRAS from Santa Cruz Biotechnology and used at 1:500; anti-p338-CRAF from Millipore and used at 1:1000.

RAS-GTP pull-down assay

RAS-GTP pull –down assay was performed according to manufacturer's protocol (Thermo Scientific #16117). Briefly, 500µg of lysates were loaded into columns together with agarose beads and RAS-RBD bait and incubated for 1 hour at 4°C. After the incubation, beads were washed three times and resuspended in LDS+Reducing agent Novex buffers (Invitrogen #NP0008, #NP0009). A fraction of lysates was used to measure total RAS amount. Pull-Down and total lysates were subjected to western blotting procedure as described above. The kit provided primary antibody against pan-RAS.

SASP Cytokine array

Conditioned media was collected from cells that were cultured in presence or absence of the drug combination. Aliquots of the media were analyzed with a multiplex immunoassay designed for human samples, "Human Cytokine Array / Chemokine Array 48-Plex HD48" (Eve technologies). Cytokine concentration was normalized by cell count.

In vivo studies

The CLR113 PDX was derived from liver metastasis. Tumour tissue was transplanted orthotopically into NSG mice to establish the PDX (IRB protocols 06-107, 14-091). Once a tumour became visible in the first mouse, it was transplanted and expanded to other animals. Tumour tissue was implanted subcutaneously in the flank of 4–6-week-old NSG female mice and treatment of the mice began when tumour reached approximately 100mm^3 in size. Mice were randomized (n = 5 mice per group) to receive drug treatments or vehicle as control.

Sotorasib (100mg/kg) and trametinib (3mg/kg) were given daily by gavage. Cetuximab was administered 50mg/kg twice a week, by intra-peritoneal injections.

Studies were performed in compliance with institutional guidelines under an IACUC approved protocol. The animals were immediately euthanized as soon as the tumours reached the IACUC set limitations.

Patients

All patients were treated on KRAS inhibitor clinical trials approved by MSKCC Institutional Review Board/Privacy Board (protocols 19-408, 20-183). Collection of patient samples were conducted under appropriate Institutional Review Board/Privacy Board protocols and waivers (protocols 06-107, 12-245, 14-019). Participating patients signed written informed consent for these clinical trials and biospecimen

protocols. This study was conducted in accordance with ethical guidelines in the Declaration of Helsinki.

Fluorescence In Situ Hybridization (FISH)

FISH analysis was performed on adherent cells. KRAS FISH analysis was performed using a 2-color KRAS/Cen12 probe mix (developed at MSKCC). The probe mix consisted of bacterial artificial chromosomes (BAC) clones containing the full length KRAS gene (clones RP11-29515 and RP11-707F18; labelled with red dUTP) and a centromeric repeat plasmid for chromosome 12 served as the control (clone pa12H8; labelled with green dUTP). Probe labelling, hybridization, washing, and fluorescence detection were performed according to standard procedures. Slides were scanned using a Zeiss Axioplan 2i epifluorescence microscope equipped with a megapixel CCD camera (CV-M4^{+}CL, JAI) controlled by Isis 5.5.9 imaging software (MetaSystems Group Inc, Waltham, MA). The entire section was scanned through 63X or 100X to assess signal pattern and select representative regions for imaging. Amplification was defined as >10 copies of each locus.

DNA sequencing

Circulating free DNA (cfDNA) Analysis

cfDNA analysis was performed using the commercially available, targeted next-generation sequencing assays Guardant360 (Guardant Health) (patients 1-5, 11) and ctDx FIRST (Resolution Bioscience) (patients 6-10). Guardant360 CDx is a CLIA-accredited, New York State Department of Health-approved cfDNA assay with analytic and clinical validation previously reported[30,31]. During this study, the assay included assessment of 74-83 genes (depending on panel version ordered) with coverage of single nucleotide variants (SNVs) and select insertions/deletions, amplifications, and fusions. Resolution Bioscience ctDx FIRST assay includes assessment of 113 genes and detects SNV/Indel Hotspots, SNV/Indel Full CDS, amplifications, deletions, gene rearrangements, and gene fusions. The ctDx FIRST assay uses a custom bioinformatics pipeline to call variants associated with genomic targets. The longitudinal ctDNA analysis in this study was performed with the Guardant360 CDx assay.

Bulk Tissue Sequencing

Genomic DNA was extracted from cell lines, frozen xenograft tumours, or formalin fixed paraffin embedded (FFPE) patient tissues obtained from biopsies or resections and sequenced with the MSK-IMPACT next-generation sequencing assay[13].

Single cell DNA sequencing

The C106-R cell line was subjected to single cell sequencing. The cell line was washed with PBS and quantified by combining 5uL of cell suspension with an equal amount of Trypan Blue, loaded on chamber slides, and counted with the Countess automated cell counter (Invitrogen). A total of 250,000 cells were used for the barcoding run. In brief, cells were encapsulated with lysis buffer (100 mM Tris at pH 8.0, 0.5%

IGEPAL, proteinase K 1.0 mg/ml) in a Tapestri platform (Mission Bio, San Francisco, CA, USA) and further lysed on the thermal cycler with the following conditions: 60 minutes at 50^{o}C and 10 minutes at 80^{o}C. The DNA from the encapsulated cell lysate was then primed and barcoded using a custom panel (Mission Bio, San Francisco, CA, USA), which targets hotspot variants of 54 oncogenes and tumour suppressor genes, for a total of 317 amplicons. After exposure to UV light, droplet PCR reactions were thermocycled with the following conditions: 6 minutes at 98^{o}C, 10 cycles of 30 seconds at 95^{o}C, 10 seconds at 72^{o}C, 9 minutes at 61^{o}C, and 20 seconds at 72^{o}C; 10 cycles of 30 seconds at 95^{o}C, 10 seconds at 72^{o}C, 9 minutes at 48^{o}C, and 20 seconds at 72^{o}C; and a final step of 2 minutes at 72^{o}C. PCR products were digested at 37^{o}C for 60 minutes and posteriorly purified using 0.63x of SPRI beads (Beckman Coulter). Sample indices and illumina adapter sequences were then added via a 9 cycle PCR reaction, and a second 0.63x SPRI purification was then performed on the completed PCR reactions. Libraries were analysed on a DNA 1000 assay chip with a Bioanalyzer (Agilent Technologies) and sequenced on a NextSeq 550 instrument (Illumina, Inc., San Diego, CA, USA; 150 bp paired-end reads). Sequence data were analysed using the proprietary software provided by Mission Bio[32]. In brief, sequence reads were trimmed for adapter sequences using Cutadapt[33] and mapped to the hg19 human genome using the Burrows-Wheeler Aligner (BWA)[34] after extracting barcode information. Following mapping, on target sequences were selected using standard bioinformatics tool (SAMtools)[35] and barcode sequences were error-corrected based on a white list of known sequences[32]. The number of cells was determined from barcodes based on number of reads assigned to each barcode and amplicon read completeness. GATK 3.7[36] was used to genotype the sample with a joint-calling approach. Genotyping calls were further examined and corrected according to variant allele frequency. For genotype clustering analysis of the two known variants (KRAS G12C and NRAS G12D), cells were included when both variants met the criteria of read depth (³10) and genotyping quality (³60). In addition, subclones having high allele dropout rate (ADO) compared to overall ADO for all cells were further excluded.

Figures

Yaeger et al. Figure 1

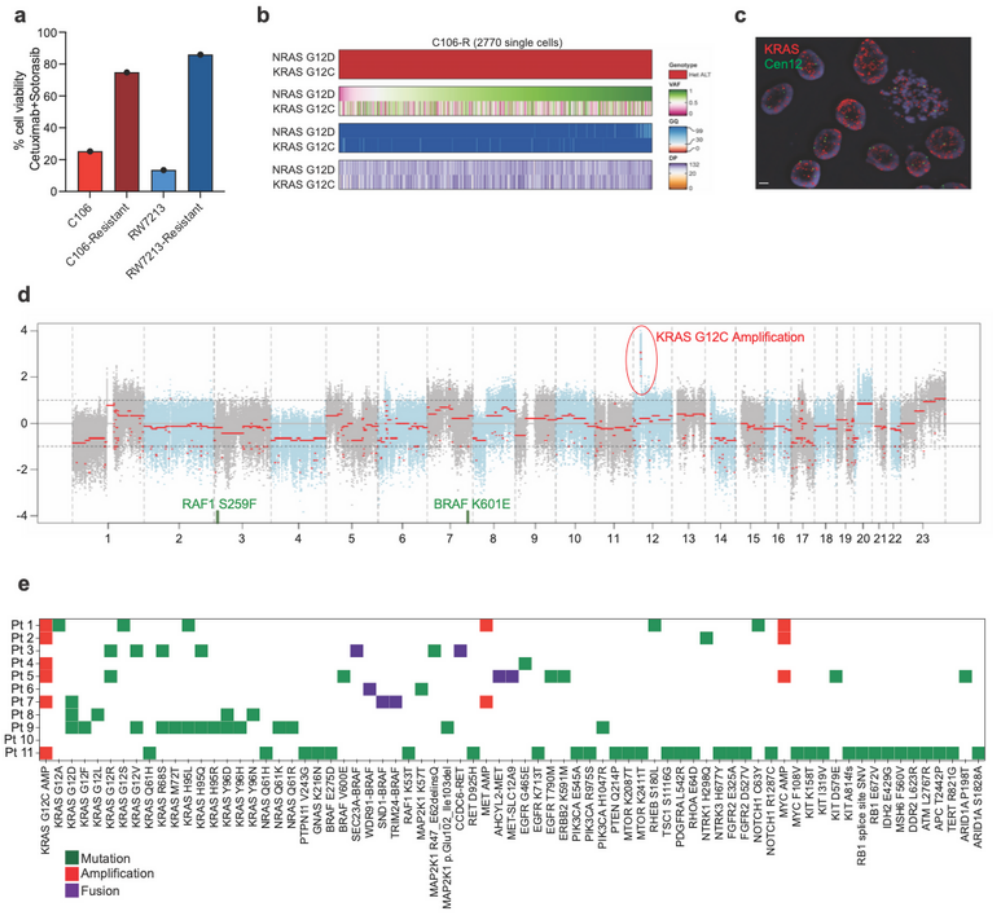

Figure 1

Mechanisms of resistance to combined KRAS G12C and EGFR inhibition in CRC. a. Graph showing cell viability of parental and resistant C106 and RW7213 cells. **b.** Heatmap of KRAS G12C and NRAS G12D alleles detected by single cell sequencing of C106 resistant subline. VAF: variant allelic frequency; GQ: genotyping quality score from GATK; DP: sequencing depth. **c.** FISH staining for KRAS gene in RW7213 resistant subline. **d.** MSK-IMPACT sequencing of resistant CLR113 PDX. **e.** Oncoprint of emergent

alterations detected in circulating tumour DNA (ctDNA) of CRC patients at time of radiographic or clinical progression through combined KRAS G12C and EGFR inhibition.

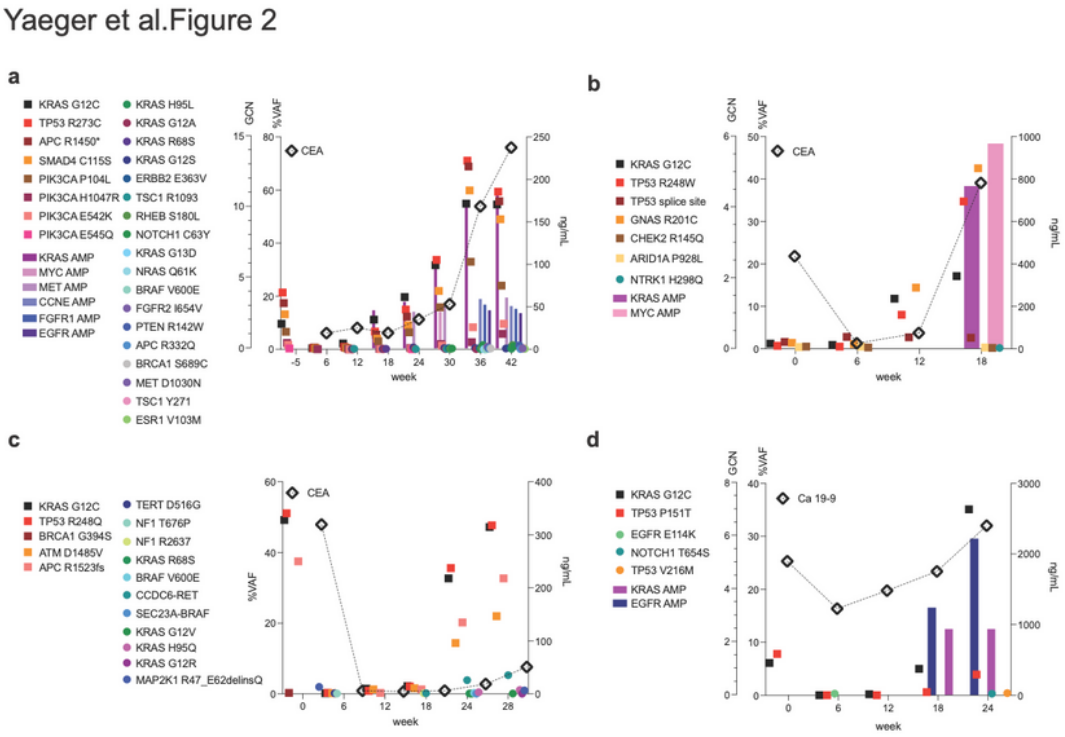

Figure 2

Longitudinal analysis of ctDNA in gastrointestinal cancer patients on KRAS G12C inhibition. a,b,c. CRC patients treated with combined KRAS G12C and EGFR inhibitors and **d.** pancreatic patient treated with

KRAS G12C monotherapy. Squares indicate alterations detectable in circulating free DNA (cfDNA) prior to treatment; circles indicate emergent alterations on treatment; bars indicate emergent copy number changes; tumour biomarker (CEA for CRC patients, Ca 19-9 for pancreatic cancer patient) indicated with a diamond. In all graphs, KRAS G12C is marked with solid black square and TP53 alterations marked with red square to track these truncal alterations.

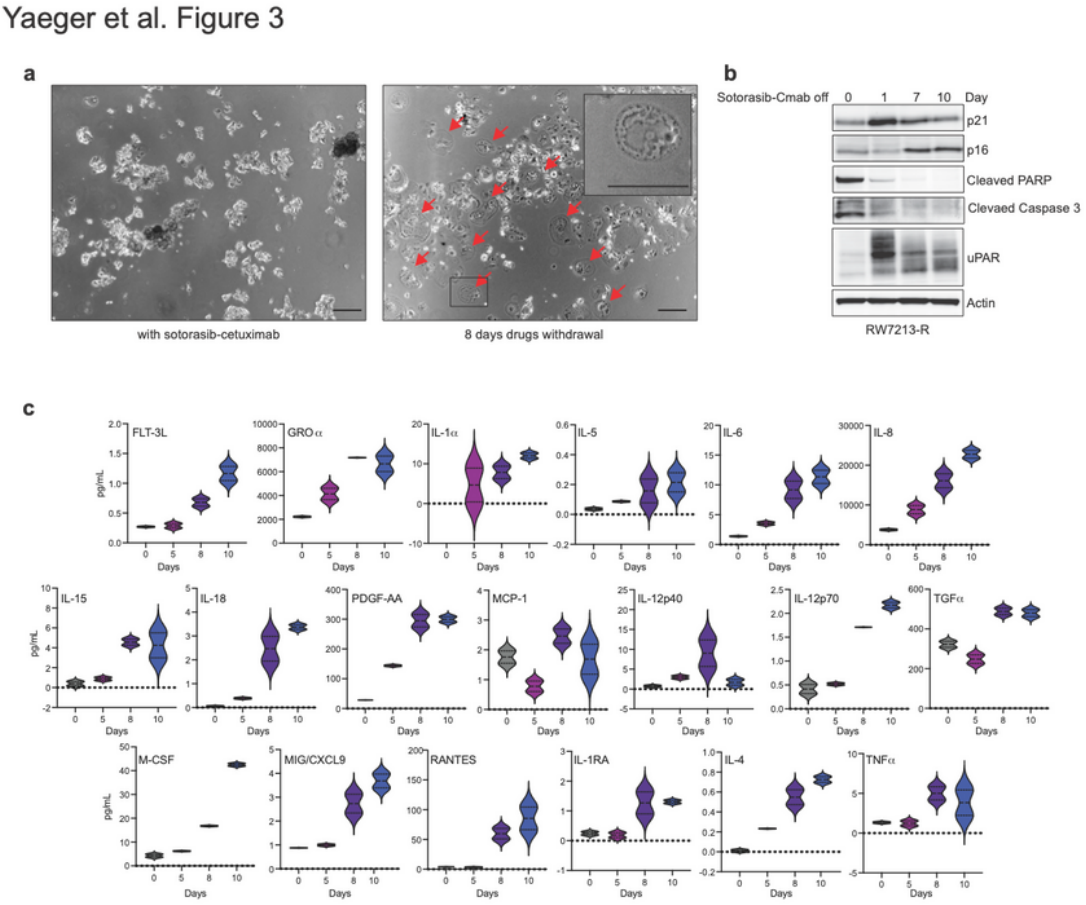

Figure 3

Drug withdrawal drives senescent phenotype in resistant CRC cell line with acquired KRAS G12C amplification. a. Microscopy images of RW7213-R with and without Cetuximab/Sotorasib combo: 10x magnification, scale bars 100mm. In the right panel, the black square represents the area magnified in the upper-right corner inset. **b**. Western blot analyses of p16, p21, caspase-3, cleaved PARP and uPAR expression upon drug withdrawal, actin is included as loading control. **c**. SASP cytokine array time course experiment. Data shown represent triplicates.

Yaeger et al. Figure 4

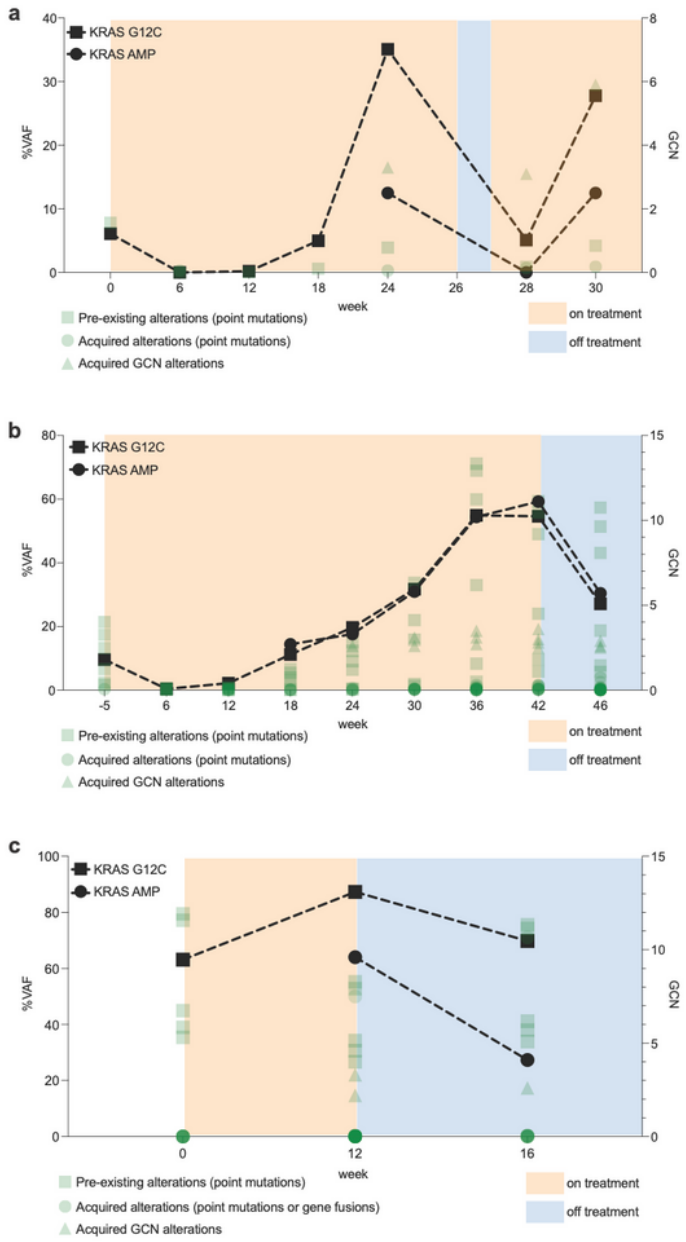

Figure 4

Effect of treatment withdrawal on amplified KRAS G12C levels in patients' circulating free DNA. a. Longitudinal analysis of ctDNA in a pancreatic cancer patient who held KRAS G12C inhibitor for eight days for toxicity. **b.** Longitudinal analysis of ctDNA in a CRC patient who held KRAS and EGFR inhibition for approximately four weeks after progression. **c.** Longitudinal analysis of ctDNA in a CRC patient who held KRAS and EGFR inhibition for approximately four weeks after progression. Orange areas indicate period of time with KRAS G12C inhibitor +/- EGFR inhibitor treatment; blue areas indicate time without KRAS G12C inhibitor and all anticancer therapy. KRAS G12C ctDNA variant allelic frequencies are marked with squares, and KRAS plasma copy numbers are marked with circles. All the other variants are reported in green.

Supplementary Files

This is a list of supplementary files associated with this preprint. Click to download.

- YaegeretalExtendedDataTable1Celllinessequencing.xlsx
- YaegeretalExtendedDataTable2PatientsCharacteristics.xlsx
- YaegeretalExtendedDataTable3PatientsCellFreeDNAdata.xlsx
- YaegeretalExtendedDataFigure1.ai
- YaegeretalExtendedDataFigure2.ai
- YaegeretalExtendedDataFigure3.ai
- YaegeretalExtendedDataFigure4.ai